The characteristic interference phenomena of wave mechanics usually can be inferred from experiment only in an indirect manner. Molecular and atomic scattering exhibit this effect directly, because the particle distribution itself is being measured. In this article, some of the qualitative features of the scattering cross-section are discussed, as well as the influence of quantum effects on the macroscopic transport properties of gases.

QUANTUM EFFECTS IN MOLECULAR SCATTERING

L. Monchick

During the first quarter of this century it became increasingly apparent that classical mechanics could not account for many of the experimental observations in atomic physics, in particular the structure of atoms and molecules and the fact that one must average over discrete states in statistical thermodynamics. There are also many experiments, not as well known, that involve the dynamics of atomic and molecular collisions and which deviate markedly from the classically predicted behavior. This article is a qualitative description of some of the effects noticed and predicted in beam-scattering experiments and in transport properties of gases at low temperatures.

In the classical description of a collision, a given set of initial positions and momenta determines a unique trajectory. As in planetary theory, the description is simplest in a frame of reference, here called the relative frame, centered on one of the two particles. The motion of the two particles is then

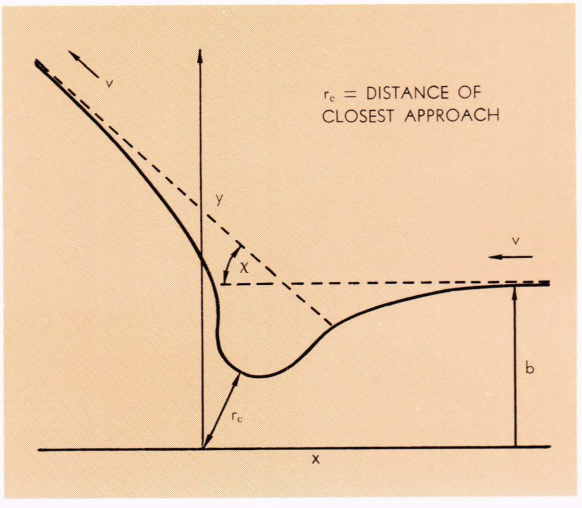

Fig. 1—Typical trajectory in a force field with both repulsive and attractive components.

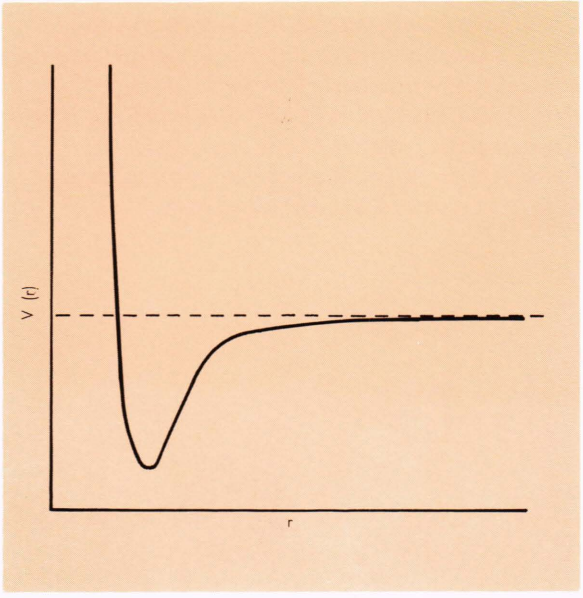

Fig. 2—Typical form of a potential energy curve, describing the interactions of neutral, spherically symmetric molecules.

equivalent mathematically to a single particle of mass $\mu = m_1m_2/(m_1 + m_2)$ moving in a field fixed at the origin of this reference frame. If in the laboratory system the initial velocities of the particles are $\mathbf{v}_1$ and $\mathbf{v}_2$, then in the relative frame the velocity of the equivalent particle is $\mathbf{v} = \mathbf{v}_1 - \mathbf{v}_2$. Figure 1 shows the trajectory of the equivalent particle in the relative frame. A particularly simple case occurs when $V(r)$, the potential energy of interaction, is a function of r only, the distance between the particles. The trajectory now will lie wholly within a plane. Although this approximation is applicable strictly only to atoms it turns out to be sufficiently accurate for many other cases. The term, r_c, is defined as the distance of closest approach achieved by the trajectory and the impact parameter, b, the corresponding distance if the interaction had been switched off. In the relative system the magnitude of the final velocity is the same as the initial velocity, but the direction of travel is rotated through an angle χ illustrated in Fig. 1 and given by

$$\chi = \pi - 2b \int_{r_c}^{\infty} \frac{dr}{r^2\left[1 - \frac{b^2}{r^2} - \frac{2V(r)}{\mu v^2}\right]^{1/2}} \quad . \quad (1)$$

Since the orbital angular momentum, **L**, is conserved by such forces, we may calculate it from the fictitious non-interacting trajectory with the result

$$\begin{aligned} \mathbf{L} &= \mu\, \mathbf{v} \times \mathbf{b}, \\ L &= \mu\, v\, b. \end{aligned} \quad (2)$$

A typical potential curve for two interacting particles is represented in Fig. 2. In Fig. 3, a deflection curve for one value of v is plotted for b lying in one plane and taking all positive values. However, in a beam experiment (where a beam of particles travelling with uniform velocity $\mathbf{v}$ is allowed to impinge on another set of particles) b may take any direction in a plane perpendicular to $\mathbf{v}$. We note that collisions with impact parameters, b_2 and b_3, but with their directions rotated through an angle of 180°, will be deflected through the same angle as b_1. From χ, as a function of b, one may now calculate $\sigma(v,\chi)\ \sin\chi\ d\chi\ d\varphi$, the relative probability of a molecule being scattered out of the beam into a given solid angle $\sin\chi\ d\chi\ d\varphi$. The term, φ, is the angle between the plane of the trajectory and some reference plane. Trajectories with their impact parameter lying in the range b, $b + db$ and φ, $\varphi + d\varphi$ will be scattered into the solid angle $\sin\chi d\chi d\varphi$. If we imagine the interaction turned off, the probability of a molecule impinging on a small element of target area, dS, is just proportional to dS for a beam of uniform intensity. Simply by requiring that everything that goes in must come out, we find

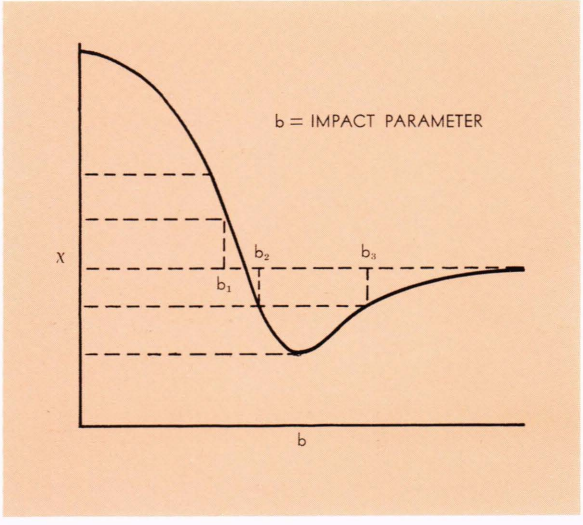

Fig. 3—Dependence of the deflection angle, χ, as a function of impact parameter, b, for a typical value of kinetic energy.

$$\sigma(v,\chi) = \sum \sigma_i(v,\chi) = \frac{1}{\sin\chi} \sum_i b_i \left|\frac{db_i}{d\chi}\right|, \quad (3)$$

where the sum runs over the several ranges of b that give rise to the same deflection angle. That the combining rule for forming σ from the separate σ_i's is simply summation, is a direct consequence of the or-or-or rule in classical probability theory.

Quantum effects can be classified mainly as interference or diffraction effects and effects due to indistinguishability. In quantum theory, one may not, as in classical theory, specify both velocity and position exactly. Instead, the maximum specification of a physical system is given by the wave function ψ. It is also termed the probability amplitude because its square, $|\psi|^2$, is the probability distribution of the positions. The or-or-or rule is now amended to read that the probability amplitudes are summed rather than the probabilities. This is sufficient to explain all the characteristic quantum interference effects. In classical theory we analyzed the total scattering as the sum of the separate scatterings of systems with all values of b, the impact parameter, or conversely, **L**, the angular momentum. In the quantum case it is still possible to specify the magnitude of the relative angular momentum of two colliding molecules. It turns out that the wave function for this case, now called the partial wave, is cylindrically symmetric about the initial direction of approach:

$$\psi_\ell = \frac{F_{k\ell}(r)}{r} P_\ell(\cos\chi)$$

$$\underset{r\to\infty}{\to} A_{k\ell} \frac{\sin(kr - \tfrac{1}{2}\ell\pi + \eta_\ell(k))}{r} P_\ell(\cos\theta) \quad (4)$$

$$L = \sqrt{\ell(\ell+1)}\,\mathrm{h} \approx (\ell + \tfrac{1}{2})\,\mathrm{h} = \mu v b$$

$$k = \mu v/\mathrm{h}$$

where ℓ is a quantum number taking integral values $0,1,2,\cdots$, P_ℓ is the ℓ'th order Legendre polynomial, η_ℓ is the phase shift, k is the wave number, and h is Planck's constant divided by 2π. The wave function will generally oscillate with the frequency of oscillation approximately proportional to the classical momentum. In a field of force the frequency will vary, being higher in the attractive part of the field and lower in the repulsive. (In Fig. 4 we have plotted schematically the frequency behavior in the absence and in the presence of an interaction.) The value, η_ℓ, is given as 2π times the difference in the total number of oscillations of the two curves as $r \to \infty$. The term, $|\psi_\ell|^2$, will in general have only a vague resemblance to the corresponding surface generated by the trajectories corresponding to some value of b. A given range b, $b + db$ for μv sufficiently large, will contain

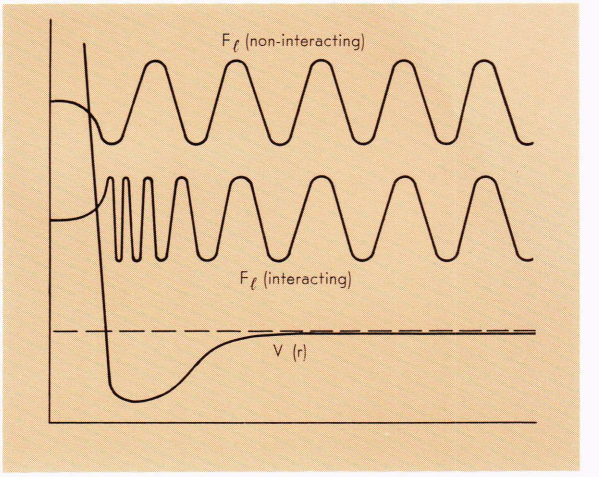

Fig. 4—Schematic behavior of frequency in presence and in absence of an interaction.

several integral values of ℓ. A wave packet may now be formed by summing the partial waves for these values of ℓ. The partial waves will interfere constructively in some regions, destructively in others, with the result that the probability distribution will resemble somewhat more closely the bundle of classical trajectories defined by b, $b + db$. As μv increases, the number of partial waves increases, and the regions of constructive and destructive interference become more sharply defined, obtaining the classical picture in the limit $\mu v \to \infty$. Another correspondence is that as μv increases, the derivative of η_ℓ with respect to ℓ approaches twice the scattering function, χ, evaluated at the impact parameter $b = (\ell + \tfrac{1}{2})\mathrm{h}/\mu v$.

Passing now to the case where all values of b, or rather ℓ, are possible we again find that for cer-

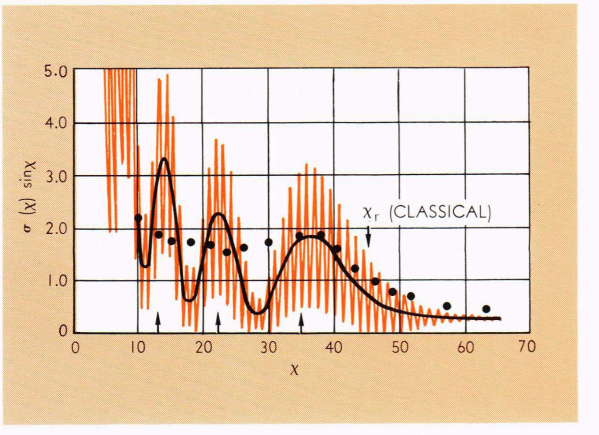

Fig. 5—Reduced differential cross-section for the scattering of a thermal molecular beam by molecules, showing primary and supernumerary rainbows.

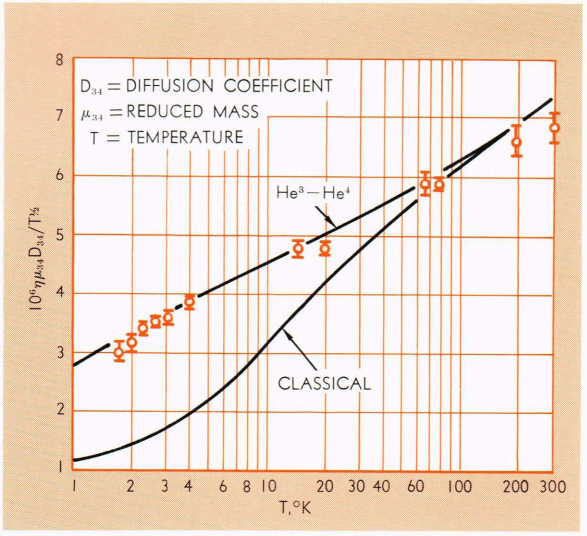

Fig. 6—Reduced diffusion coefficients of a He^3-He^4 mixture from 2°K to room temperature. See Ref. 2. The smooth curves are the theoretical predictions.

tain values of $\chi \leq |\chi_r|$, three small separated ranges of ℓ contribute to the scattering. For μv in the range of interest in molecular scattering, these will approximate the classical values of b for the same χ. Instead of the intensities, as in the classical case, we add the amplitudes, with the result that interference effects lead to a new formula for scattering (for high molecular weights or energies):

$$\sigma(\chi,v) = \sum_i \sum_j [\sigma_i(v,\chi)\,\sigma_j(v,\chi)]^{1/2} e^{i(\beta i - \beta j)}$$

$$\beta \equiv \left[2\eta_\ell - 2(\ell + \tfrac{1}{2}) \frac{\partial \eta_\ell}{\partial \ell} - \left(2 - \frac{\partial^2 \eta_\ell}{\partial \ell^2} \Big/ \left| \frac{\partial^2 \eta_\ell}{\partial \ell^2} \right| - \frac{\partial \eta_\ell}{\partial \ell} \Big/ \left| \frac{\partial \eta_\ell}{\partial \ell} \right| \right) \frac{\pi}{4} \right].$$

Figure 5 shows a typical plot of σ versus χ. In an experiment with the resolving power commonly available, the fine oscillations will be averaged out to yield the more slowly oscillating curve. The calculations are for a Lennard-Jones (12-6) potential with parameters corresponding approximately to K-HBr, for which experimental points at low resolution are shown. The arrows show the semiclassical prediction of the classical rainbow edge (45°), the first maximum (35°), the first minimum (22°), and the second maximum (13°). See Ref. 1.

The smooth curve bisecting the rapidly oscillating curve is presumably what would be observed in an apparatus of low resolution. The rainbow angle, so called because the mathematical theory resembles very closely the theory of light scattering by raindrops, is identified as χ_r. The hump centered just to the left of χ_r has been seen many times and is even approximately predicted by classical theory. The secondary peaks to the left are predicted only by the quantum theory and also have an analog in light scattering theory where they are called supernumerary rainbows. Experimental data plotted in Fig. 5 seem to give a slight indication of one such peak. Since this experiment, others have been performed exhibiting three or four supernumerary rainbows and even some of the fine structure.

Quantum effects appearing in the transport properties of gases are not as spectacular as those exhibited by molecular scattering because the transport coefficients themselves turn out to be averages of certain functions of the molecular velocities, v, and the scattering angle, χ, over all possible collisions. Most of the oscillatory nature of σ will be averaged out. It may be shown that at ordinary temperatures, μv, which is proportional to $T^{1/2}\mu^{1/2}$ on the average, is sufficiently large that quantum effects are small. (T is the temperature.) But this is not the case for He^3 and He^4 below room temperature. From measurements of the nonideality of He^4 at high temperatures the potential

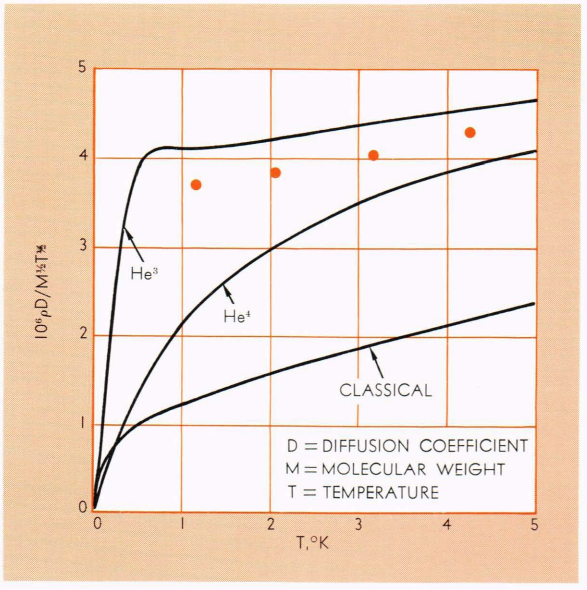

Fig. 7—Reduced self-diffusion coefficients of He^3. See Ref. 2. The smooth curves are the theoretical predictions.

[1] E. A. Mason and L. Monchick, "Supernumerary Rainbows in Molecular Scattering," *J. Chem. Phys.* **41**, Oct. 1964, 2221-2222.

[2] L. Monchick, E. A. Mason, R. J. Munn, and F. J. Smith, "Transport Properties of Gaseous He^3 and He^4," *Physical Review*, **139**, Aug. 16 - Sept. 27, 1965, A1076-A1082.

energy is known fairly accurately. We have assumed that this potential is unchanged for He^3-He^3 and He^3-He^4 interactions and have used it to calculate the properties described below.

In a mixture of two experimentally distinguishable atoms the binary diffusion coefficient is almost wholly a function of the interaction between the unlike atoms. Measurements in He^3-He^4 mixtures and spin diffusion measurements in He^3 allow us a test for our theory. A comparison of the quantum and classical calculations for He^3-He^4 and the experimental results is presented in Fig. 6. The He^3 nucleus has a spin of ½, which in a suitable spin resonance experiment may be partially oriented. If the time to diffuse from one region to the other is short compared with the natural flip-over time of the spins, atoms with different spins may be regarded as distinguishable and the interdiffusion measured. Calculations for this system are presented in Fig. 7 and contrasted with experiment.

In a gas consisting of either pure He^3 or pure He^4 the fact that we have to deal with collisions between indistinguishable particles introduces a new complication. The Pauli exclusion principle states that the wave function of a system changes sign whenever two like fundamental particles are interchanged. Since He^4 has even numbers of electrons, protons, and neutrons, the interchange of He^4 atoms leaves the wave function unchanged. The partial wave changes sign (or is antisymmetric) when ℓ is odd; it is unchanged (or symmetric) when ℓ is even. This means that in describing the collision of two He^4 atoms odd values of ℓ are excluded.

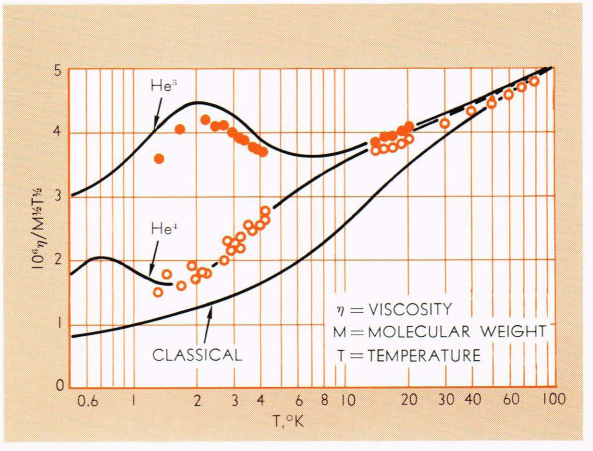

Fig. 8—Reduced viscosity of helium isotopes. See Ref. 2. The smooth curves are the theoretical predictions.

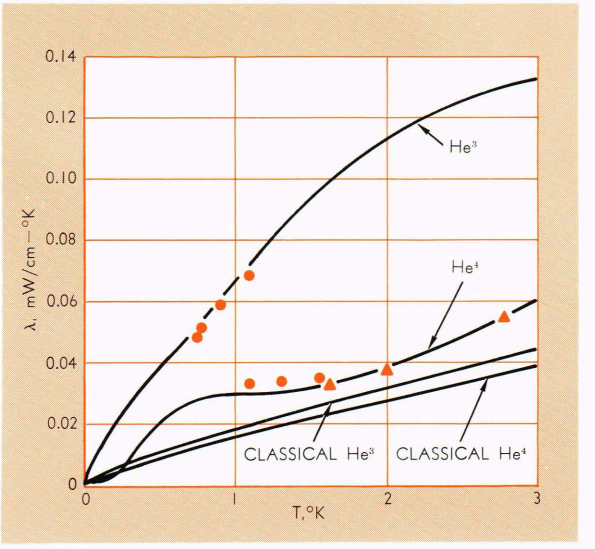

Fig. 9—Reduced thermal conductivity of helium isotopes. See Ref. 2. The smooth curves are the theoretical predictions.

Since He^3 has an odd number of neutrons the total wave function must be antisymmetric with respect to exchange of He^3 atoms. From the separate spin functions of the nuclei, it is possible to construct one symmetric and three antisymmetric spin angular momentum eigenfunctions. This is quite similar to the way in which one constructs the ${}^1\Sigma g^+$ and ${}^3\Sigma u^+$ states of H_2. Now, the even values of ℓ combine with antisymmetric spin function, the odd values with the three symmetric spin functions. Thus, although the potential energy of He^3 atoms may be the same as that of He^4, over and above the differences due to the difference in atomic weight, we may still expect the scattering patterns in the two gases to be qualitatively different. This is particularly evident at low temperatures, where only small values of ℓ are important, as can be seen from the comparison of theory and experiment for viscosity and thermal conductivity in Figs. 8 and 9.

It should be evident from the preceding that the transport properties of He^3 and He^4 can be calculated with the same potential function as was found experimentally at high temperatures if suitable account is taken of quantum effects. Classical theory, as was expected, failed miserably. One effect not discussed in this article is quantum mechanical tunnelling. This was taken into account in the calculations but did not produce more than a small correction in the final results.